ELSEVIER

Thermochimica Acta 367–368 (2001) 203–215

thermochimica acta

www.elsevier.com/locate/tca

Multi-frequency sawtooth modulation of a power-compensation differential scanning calorimeter☆

Y.K. Kwon[a,b], R . Androsch[a,b,1], M. Pyda[a,b], B. Wunderlich[a,b,*]

[a]*Department of Chemistry, University of Tennessee, Knoxville, TN 37996-1600, USA*

[b]*Oak Ridge National Laboratory, Chemical and Analytical Sciences Division, Oak Ridge, TN 37831-6197, USA*

Received 15 October 1999; accepted 1 May 2000

Abstract

In this paper experiments with temperature-modulated differential scanning calorimetry (TMDSC) are described in which the modulation consists of multiple, superimposed frequencies. The harmonics of the Fourier series of the measured heat-flow rate and temperature are deconvoluted to extract data pertaining to the different frequencies. In order to derive 1st, 3rd, 5th, and 7th harmonics of similar amplitudes, a complex, but simple-to-program sawtooth is generated. In TMDSC with sawtooth modulation with a period of less than about 150 s, a correction by extrapolation to zero frequency is necessary. It is shown that the extrapolation of the heat capacity calculated from the amplitudes of the first and higher harmonics of the Fourier-transforms of heat-flow rate and the sample temperature permits this evaluation of the heat capacity from a single experiment. The method is tested on a power-compensation type TMDSC with temperature control close to the calorimeter heater. The time constant for the response of the calorimeters is less than 30 s ($\tau < 5\,\mathrm{s\,rad^{-1}}$). Instabilities of the calorimeter response are removed by smoothing. Published by Elsevier Science B.V.

Keywords: Heat capacity; Temperature-modulated differential scanning calorimetry; TMDSC; Fourier transformation; Higher harmonics; Sawtooth modulation

1. Introduction and computation method

In temperature-modulated differential thermal analysis (TMDSC) a modulation program is produced by superposition of a constant heating rate, $\langle q \rangle$ of perhaps 0.5–5.0 K min^{-1} and a temperature-modulation with an amplitude A_{T_s} of 0.1–5.0 K at a frequency ω of between 0.02 and 0.20 rad s^{-1} [1,2]. The common modulations are sinusoidal or sawtooth-like. For measurements of heat capacities, quasi-isothermal TMDSC with $\langle q \rangle = 0$ is most precise.

Measurements of heat capacity with a power-compensated instrument were shown recently to need data at different frequencies to remove the frequency-, sample-, and mass-dependence of the evaluations at modulation periods of less than about 150 s [3,4]. To reduce the time needed to perform multiple experiments, we turned to the study of a different frequencies in the same experiment. Such simultaneous use of

* Corresponding author. Present address: Department of Chemistry, University of Tennessee, Knoxville, TN 37996-1600, USA.
E-mail address: athas@utk.edu (B. Wunderlich).

[1] Present address: Martin-Luther-University Halle-Wittenberg, Institute of Materials Technology, Geusaer Str., 06217 Merseburg, Germany.

0040-6031/01/$ – see front matter Published by Elsevier Science B.V.
PII: S0040-6031(00)00695-X

multiple modulation frequencies was proposed already at the outset of TMDSC [5], but as far as we are aware of, has not yet been routinely applied to TMDSC. To provide such measurements, we used the different harmonics generated by a centrosymmetric sawtooth for the evaluation of the data at different frequencies [6]. Although, the method was quite successful, increasingly higher harmonics of a sawtooth have lower amplitudes and, thus, are expected to lose on precision. In a further development, we designed a complex sawtooth with close to equal amplitudes for the 1st, 3rd, 5th, and 7th harmonic [7]. In this paper, the application of such modulation to a Perkin-Elmer Pyris-1 DSC (DDSC^{TM}) will be explored.

The relationship between the amplitudes of the heat-flow rate $A_{HF}(v)$ and the sample temperature $A_{T_s}(v)$ is given by [6]

$$C_p = \frac{A_{HF}(v)}{A_{T_s}(v)} \frac{1}{v\omega} \sqrt{1 + \tau^2 (v\omega)^2} \quad (1)$$

where v is the integer characterizing the harmonic to be analyzed, and τ a constant whose dependence on the various run parameters needs to be evaluated to compute the heat capacity C_p. With at least four values of v, a corrected C_p can be found at zero frequency by extrapolation from a plot of $[A_{HF}(v)/A_{T_s}(v)v\omega]^{-2}$ versus ω^2.

After the C_p is known for the sample, a reference material (usually sapphire, Al_2O_3), and a baseline run of two empty calorimeter pans is carried out at the same temperature, T_o, so that the calibrated sample heat capacity can be evaluated by subtracting or adding the baseline heat capacity. This process corrects for calorimeter asymmetry from the sample and reference heat capacities. Finally, the sample heat capacity is adjusted with the same calibration factor needed to get agreement of the literature value for sapphire [8] with the measured reference value. Usually, the heat flow of the calorimeter is first approximately calibrated with the heat of fusion of indium, so that the just described final calibration is less than 10%.

Often the baseline correction is carried out by subtracting the heat-flow rate of the baseline in the time domain instead of subtraction of the heat capacity calculated from the baseline run, an option in the software of many calorimeters, and a convenient practice also applied in the present work. It was shown recently, however, that baseline subtraction in the time domain is mathematically not sound and introduces a (small) nonlinearity into the measurement. It is thus suggested that the method described in the previous paragraph should be used for higher frequencies and when precision is to approach the 1% mark [7].

Table 1
Approximate complex sawtooth program for $\omega = 210$ s

Segment No.[a]	Time (s)	Amplitude (K)
1	0–7.5	0.0–1.0
2	7.5–22.5	1.0–0.0
3	22.5–37.5	0.0–0.5
4	37.5–52.5	0.5–0.0
5	52.5–67.5	0.0–0.5
6	67.5–82.5	0.5–0.0
7	82.5–97.5	0.0–1.0
8	97.5–112.5	1.0 to −1.0
9	112.5–127.5	−1.0–0.0
10	127.5–142.5	0.0 to −0.5
11	142.5–157.5	−0.5–0.0
12	157.5–172.5	0.0 to −0.5
13	172.5–187.5	−0.5–0.0
14	187.5–202.5	0.0 to −1.0
15	202.5–210.0	−1.0–0.0

[a] Note that in order to keep a centrosymmetric sawtooth, segments 1 and 15 are half segments.

Using the complex, centrosymmetric, sawtooth-like temperature-modulation listed in Table 1 about the temperature T_o, as carried out in quasi-isothermal TMDSC [9,10], one obtains, e.g. the following first five harmonics [7]:

$$T(t) - T_o = A[0.379 \sin \omega t - 0.251 \sin 3\omega t + 0.217 \sin 5\omega t - 0.348 \sin 7\omega t + 0.067 \sin 9\omega t - \cdots] \quad (2)$$

which are shown in Fig. 1, together with their sum. Higher harmonics are not shown in the figure, but decrease rapidly with v. Each half sub-segment of the 210 s sawtooth is 15-s long and the harmonics with $v = 1$, 3, 5, and 7 correspond to the periods p of 210, 70, 42, and 30 s. The 9th harmonic with a period of $23\frac{1}{3}$ s is used for reference and has a lower amplitude, although it is enhanced over that of a simple sawtooth by a factor 8 [7].

Since this analysis is a single-run measurement, it could be included in the software for data treatment,

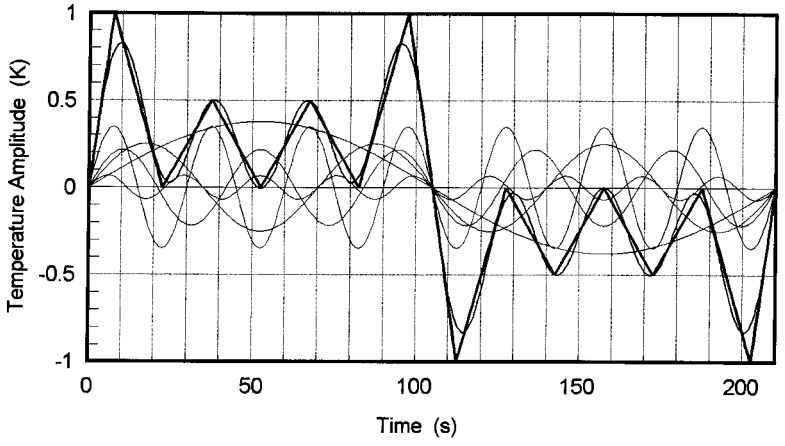

Fig. 1. Programmed temperature for the complex sawtooth given in Table 1 for a modulation period p of 210 s and its harmonics $v = 1, 3, 5, 7,$ and 9 (thin lines) and their sum (intermediate line).

together with the extrapolation to zero frequency of Eq. (1), suggested above. Furthermore, the 14 segments of the complex sawtooth are sufficiently simple to be programmed with any high-quality, standard DSC and repeated continually for TMDSC. For TMDSC with an underlying rate of temperature change, $\langle q \rangle$, the required temperature increase or decrease must be added to the complex sawtooth.

2. Experimental details

2.1. Instrumentation

A commercial Perkin-Elmer PYRIS-1 DSC system was used for all measurements. It was equipped with a liquid nitrogen accessory. Temperature calibrations were done with the melting transitions of indium (429.75 K) and cyclohexane (s/s 186.09 and s/l 297.7 K) at a heating rate of 10 K min^{-1}. The onsets of the first-order transitions were determined by the extrapolation of the leading edge of the transition peaks to the baseline. The change of the calibration with heating-rate was determined earlier to be about 0.03 K per K min^{-1} [12] and is considered negligible for the present application for the determination of heat capacities. The heating rates of up to ± 8 K for the complex sawtooth of 210 s in Table 1 introduce errors in the quoted temperatures of less than 0.5 K. A preliminary heat-flow-rate calibration was carried out with the heat of fusion of indium. The final calibration of the heat-flow rate with 22.14 mg of sapphire (Al_2O_3) was undertaken by the special procedure, discussed above, but the comparison of the data was carried out with the frequency-corrected, uncalibrated data of polystyrene. Helium with a flow rate of 20 ml min^{-1} was purged through the cell. The helium decreases the thermal resistance between sample, pan, and the base containing both heater and thermometer. Note that the use of helium is questionable in the heat-flux DSC, since there the benefits just listed, are offset by increased direct heat conduction through the gas phase from the heater and reference without benefit of the controlled path of heat flux.

2.2. Multifrequency sawtooth modulation

The quasi-isothermal complex sawtooth modulation followed the thermal program of Table 1. In another set of experiments, we used a period, p, of 420 s to follow the influence of p on the harmonics of the Fourier series. The length of each sub-segment for the complex sawtooth with $p = 420$ s is 30 s and the periods for the harmonics with $v = 1, 3, 5, 7,$ and 9 are 420, 140, 84, 60 and $46\frac{2}{3}$ s, respectively. To achieve statistically significant averages, at least five cycles of the modulation were repeated for each result. Experiments were made on atactic polystyrene (MW = 280,000) with two different sample masses (6.785 and 15.900 mg) and two empty aluminum pans

as a baseline run. The pan weights were always about 23 mg. The heat flow rate of the baseline run was subtracted from the sample run in the time domain, correcting only approximately for the asymmetry of the equipment, as discussed in Section 1. In the future, for high-precision applications, the here displayed measurements are to be improved by subtraction of the heat capacity of the baseline run after establishing its sign instead of the baseline subtraction in the time domain, and carrying out a calibration run alongside every sample and baseline run. In the present set of experiments this full protocol was not felt to be necessary, since the data-bank information on the heat capacity of polystyrene is not known to be better than ±3% [14].

2.3. Data treatment

The experimental data, consisting of heat-flow rates after baseline-correction in the time domain and sample temperatures as a function of time at the various base temperatures, were used for analysis outside the software provided by the manufacturer. A typical example of one cycle of such data is shown in Fig. 2 and curve (b) should be compared to Fig. 1. Due to a non-instantaneous response of the DSC under the programming conditions, the observed heat flow data in curve (a) contain sharp spikes at the end of every sub-segment, as is frequently observed. But, as can be seen in the prior experiments with the same calorimeter [3,4,6], calibration and adjustment of samples and references can minimize this effect.

When treating the data without correction for the spikes, errors arise in the heat capacity, since the temperature modulation has no corresponding effect. The fit of a Fourier series produces larger, higher harmonics to account for the more complicated shape. To reduce these instrumental artifacts, the raw data of the heat flow rate were smoothed by averaging each data point with the nearest and next-nearest neighbors (five-data-point average). This smoothing procedure was repeated three times before further calculations were undertaken. Fig. 3 illustrates the effect of the successive smoothing on a single sawtooth. It is obvious from the figure that the smoothing does not change the total heat flow of the response to the modulation, but removes the artifacts.

The calculation of the harmonics of the Fourier series and the evaluation of the heat capacity, C_p, was programmed in Mathematica 3.0™, i.e., none of the modulation and computation capabilities of the DDSC™ were made use of, and any traditional DSC can be used for similar experimentation.

Fig. 2 shows that for this experiment every segment of the complex sawtooth reaches steady state in the heat-flow rate, indicated by the horizontal portion of

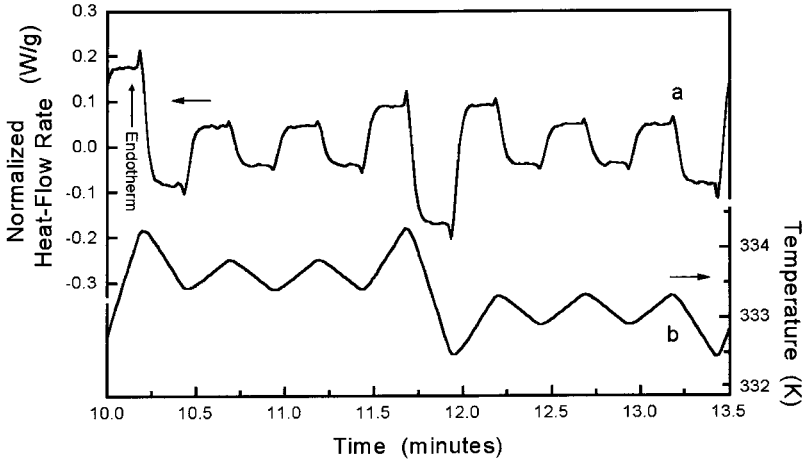

Fig. 2. Example of a complex sawtooth modulation of Table 1 with the Perkin-Elmer Pyris-1. The maximum amplitude A_{T_s} is 1.0 K, T_o is chosen to be 335.5 K, the period $p = 210$ s, the sample is polystyrene with a mass of 6.785 mg. The data are plotted after subtracting the empty–empty run in the time domain.

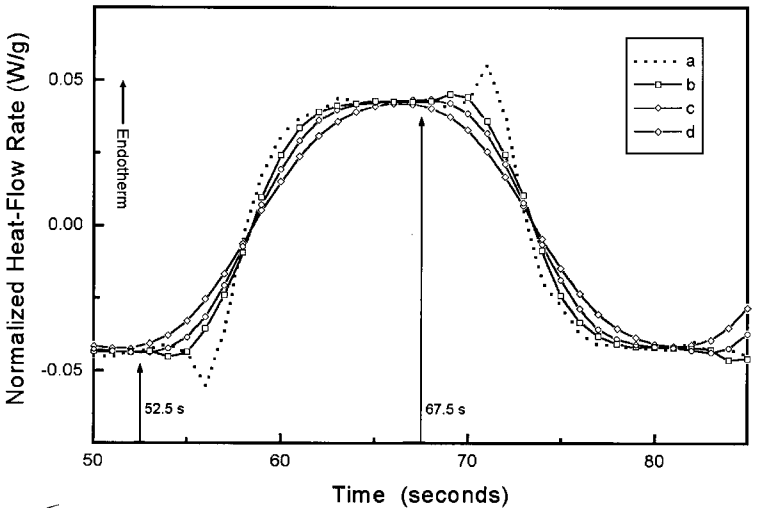

Fig. 3. Change of the heat-flow rate in a section of the curve of Fig. 2 on smoothing. (a) Curve of the measured heat-flow rate, (b) curve of the smoothed data by averaging five data points of (a), (c) curve of the data that were smoothed twice, (d) curve of the data that were smoothed three times.

the curve. These heating and cooling sub-segments with constant heating rates, q, were, thus, also used to calculate the heat capacities using the analysis method for the standard DSC ($C_p \approx K\,\mathrm{HF}/q$) [13]. Prior to this calculation, the heat-flow data within the regions of steady-state were also smoothed to minimize the statistical fluctuations. Furthermore, the corresponding smoothed heat flow data were averaged using two cycles of the sawtooth modulation.

3. Results

3.1. Effect of smoothing

An initial analysis of the heat-flow rate and sample temperature responses was done on the data for 6.885 mg of polystyrene of Fig. 2 without smoothing. The amplitudes of the sinusoidal Fourier components are collected in columns 3 and 4 of Table 2. Due to the

Table 2
Amplitudes of the Fourier Components of the sample temperature, heat-flow rate, and the calculated heat capacity for polystyrene ($p = 210$ s, 6.785 mg, $T_o = 333.65$ K)

Harmonics		$A_{HF}(v)$ (W g^{-1})	$A_{T_s}(\upsilon)$ (K)	C_p [a]
1st	2nd period	0.014525	0.37755	1.28582
	3rd period	0.014586	0.37793	1.28992
2nd	2nd period	1.65×10^{-4}	6.25×10^{-4}	–
	3rd period	1.93×10^{-4}	4.32×10^{-4}	–
3rd	2nd period	0.029130	0.24894	1.30365
	3rd period	0.029095	0.24905	1.30152
5th	2nd period	0.041415	0.21216	1.30486
	3rd period	0.041507	0.21219	1.30757
7th	2nd period	0.091892	0.33179	1.32239
	3rd period	0.091924	0.33181	1.32277
9th	2nd period	0.022620	0.06617	1.36202
	3rd period	0.022485	0.06234	1.33955

[a] Uncorrected specific heat capacity of Eq. (1) with $\tau = 0$, in J K^{-1} g^{-1}.

centrosymmetric nature of the complex sawtooth and the heat-flow rate response, there are practically only odd-numbered harmonics. Furthermore, it can be seen that the amplitudes are repeatable from the second cycle on.

The heat capacity was calculated from Eq. (1) for the various harmonics and plotted as a function of p/v setting initially $\tau = 1.0$ and is listed in the last column of Table 2. Obviously, there is a frequency dependence of the heat capacity. But, when compared with the prior analyses with a single sawtooth [3,4,6], the heat capacities increase with frequency, rather than decrease. This increase of heat capacity with frequency is mainly due to the distorted shape of the heat-flow rate in Fig. 2 and can be taken as an example of the influence of a nonlinear response in the time interval of switching the rate of temperature change.

To eliminate these instrumental effects without changing the integral heat flow, the raw data were smoothed, as described in Section 2. Once smoothed, the sharp corners disappear, as illustrated in Fig. 3. Fig. 4 shows the changes in heat capacity with frequency as calculated from the smoothing steps of Fig. 3, and Fig. 5 represents a plot of the inverse, squared, uncorrected heat capacity versus the frequency square. Such a plot was shown in [3,4] not only to establish the true heat capacity at zero frequency, but also indicate the region of independence of τ from frequency. From curve d, a value of $\tau = 3.01\,\mathrm{s\,rad^{-1}}$ is obtained. The value of τ was found earlier to depend on sample type, mass, and even on the positioning of the calorimeter pans, but over a reasonable range does not depend on the modulation period (down to about 10 s) [3,4,6]. In Fig. 5, the slope increases with smoothing, illustrating another influence on τ, namely, that of the control of the heaters in a power-compensation DSC.

After smoothing, the Fourier amplitudes approach values that appear reasonable. Table 3 summarizes the amplitudes of the various harmonics of the Fourier-transforms of the smoothed heat-flow rates (curve, d, in Figs. 3–5) and the corresponding sample temperatures which were not smoothed, and remain as in Table 2. The average, corrected heat capacity calculated from the last column of Table 3 with the help of the value of $\tau = 3.01\,\mathrm{s\,rad^{-1}}$ is $1.30 \pm 0.7\%\,\mathrm{JK^{-1}\,g^{-1}}$. Since a better fit between data and sum of the Fourier components was obtained by smoothing, all further data are smoothed before calculation.

3.2. The effect of change of the modulation period, sample mass, and temperature

Fig. 6 represents a comparison of heat-flow rates for a larger polystyrene sample (15.900 mg) using two different overall modulation periods. The modulation

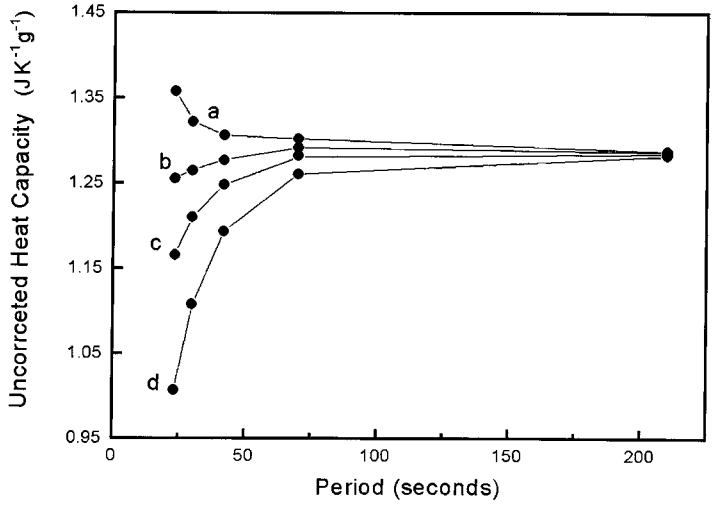

Fig. 4. Change of the uncorrected heat capacities with the degree of smoothing. The labeled curves refer to different degrees of smoothing, as in Fig. 3.

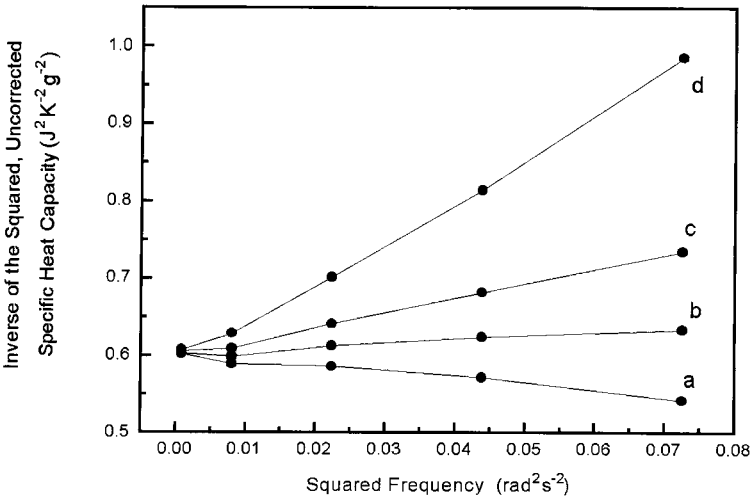

Fig. 5. Plot of the uncorrected heat capacities calculated from the variously smoothed heat-flow rates as suggested by Eq. (1). Curves a–d refer to different degrees of smoothing as in Fig. 3.

with a period of 420 s reaches a steady state for up to 30 s, with 210 s, it barely reaches steady state. In this figure, the fit between the observed heat-flow rate and the sum of the first to the 9th harmonic was better for the period of 210 s because it resembles a sinusoidal modulation response. The uncorrected data in Fig. 7 (● and ■, for $p = 210$ and 420 s, respectively) illustrate the changes in the uncorrected, apparent specific heat capacity with frequency when using Eq. (1) with $\tau = 0$. A linear regression fitting of the data of Fig. 7 when plotted as inverse square versus the square of the frequency is shown in Fig. 8 and leads to τ values (slopes) of 3.06 and 4.94 s rad^{-1}, respectively.

Next, we measured the heat-flow rates and sample temperatures of the complex sawtooth modulation on 0.6785 mg of polystyrene at different temperatures throughout the glass transition region. Fig. 9 shows the change of the uncorrected (filled symbols) and corrected heat capacities (open symbols) with frequency at the respective temperatures and frequencies. The

Table 3
Amplitudes of the Fourier components of the sample temperature, heat-flow rate, and the calculated heat capacity for polystyrene after smoothing[a] as shown in Fig. 3

Harmonics		A_{HF} (W g^{-1})	$A_{T_s}(v)$ (K)	C_p [b]
1st	2nd period	0.014303	0.37755	1.28197
	3rd period	0.014697	0.37793	1.28390
2nd	2nd period	1.71×10^{-4}	6.25×10^{-4}	–
	3rd period	1.82×10^{-4}	4.32×10^{-4}	–
3rd	2nd period	0.028908	0.24894	1.26284
	3rd period	0.028867	0.24905	1.25974
5th	2nd period	0.040517	0.21216	1.19310
	3rd period	0.040590	0.21219	1.19493
7th	2nd period	0.087945	0.33179	1.10811
	3rd period	0.087962	0.33181	1.10022
9th	2nd period	0.021040	0.06617	1.01605
	3rd period	0.020904	0.06234	0.99830

[a] The smoothed data were obtained by three successive averages, as described in Section 2.
[b] Uncorrected specific heat capacity of Eq. (1) with $\tau = 0$, in J K^{-1} g^{-1}.

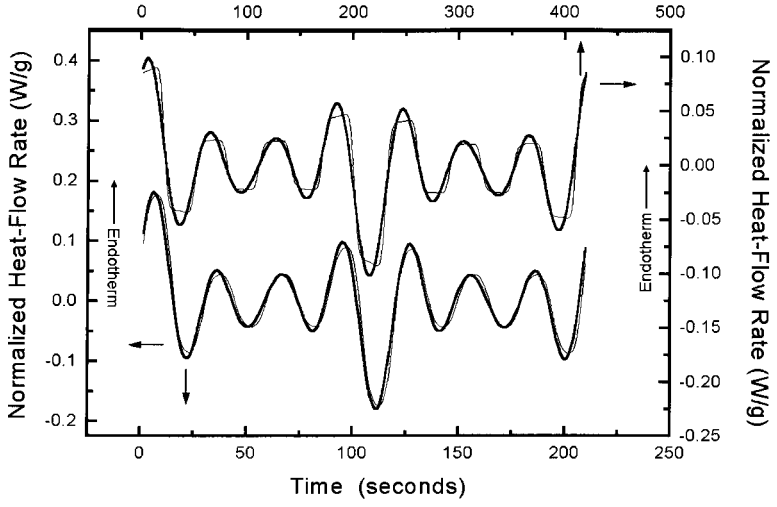

Fig. 6. Heat-flow rates for polystyrene with a mass of 15.900 mg at overall modulation periods of 210 s (lower curves) and 420 s (upper curves). The heavier curves represent the sums of the used harmonics with odd v from 1 to 9.

corrected heat capacities in the solid and liquid states are 1.3022, 1.7617, and 1.9070 J K^{-1} g^{-1} at 333.65, 373.65, and 413.65 K, respectively. The corresponding values of τ were 3.01, 3.31, and 3.38 s rad^{-1}, revealing only a gradual change.

The specific heat capacities are close to those of the ATHAS data bank [14]. The recommended heat capacity of the glassy polystyrene at 333.65 K is 1.379 J K^{-1} g^{-1}, and that of the liquid at 413.65 K is 1.970 J K^{-1} g^{-1}, and, as expected, the heat capacity within the glass transition region is intermediate. The data bank data are expected to be accurate to about $\pm 3\%$, and the newly measured sample would still have to be calibrated with sapphire.

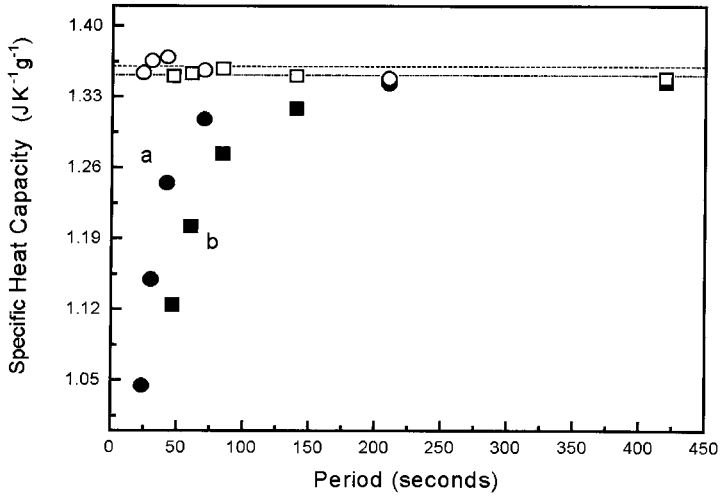

Fig. 7. Comparison of the heat capacities of 15.900 mg of polystyrene, analyzed with two different frequencies as seen in Fig. 6 and calculated using Eq. (1). Filled circles uncorrected specific heat capacities (setting $\tau = 1.0$). The corrected heat capacities with a τ obtained by linear fitting, as illustrated in Fig. 8, are indicated by the open symbols.

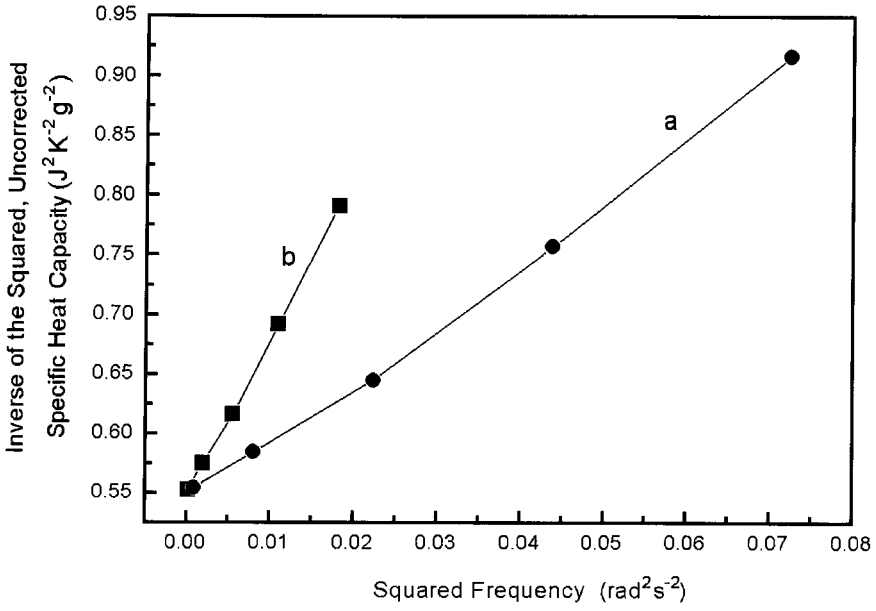

Fig. 8. Extrapolation of the apparent heat capacities of Fig. 7 to zero frequency for the various harmonics. Curve (a) for a p of 210 s, curve (b) for a p of 420 s.

3.3. Calibrations with sapphire and by standard DSC and Lissajous figures of the complex sawtooth

A Sapphire sample of 22.14 mg was analyzed using a period of $p = 210$ s, and led to a corrected specific heat capacity of 0.8661 J K^{-1} g^{-1} at 333.65 K with a value of τ for Eq. (1) of 3.8 s rad^{-1}, compared to the literature value of 0.8429 J K^{-1} g^{-1} [8]. The correction factor to true heat capacities at 333.65 K is, thus 0.9732, but is not applied to the polystyrene data since

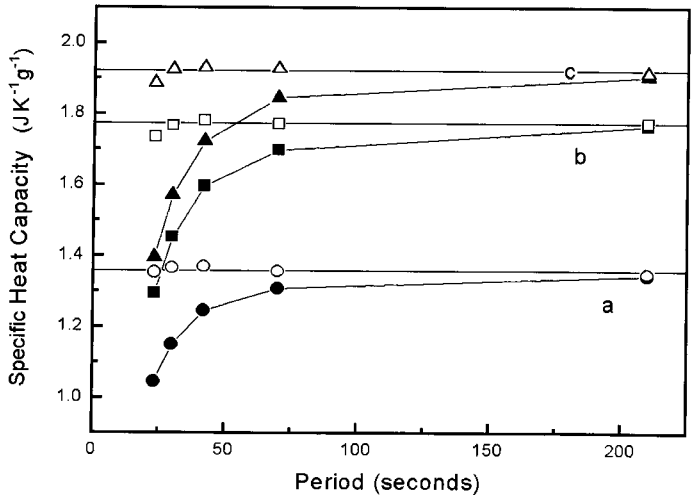

Fig. 9. Comparison of the heat capacities of polystyrene at different temperatures. The uncorrected, apparent heat capacities are given by the filled symbols, the corrected values by the open symbols. The overall p is 210 s and the sample mass is 15.900 mg. Curves a, b, and c refer to the temperatures 333.65, 373.65, and 413.65 K, respectively.

Table 4
Calculation of the heat capacity of polystyrene at 333.65 K by standard DSC[a]

Sample (mg)	Period p (s)	$\langle q \rangle$ (K min^{-1})	$\langle$HF$\rangle$ (W g^{-1})	C_p (J K^{-1} g^{-1})
6.785	210	8	0.1732	1.2988
		4	0.0869	1.3041
		2	0.0442	1.3260
	420	4	0.0940	1.4096
		2	0.0466	1.3982
		1	0.0238	1.4297
15.900	210	8	0.1769	1.3243
		4	0.0873	1.3099
		2	0.0439	1.3172
	420	4	0.0925	1.3874
		2	0.0463	1.3874
		1	0.0231	1.3885

[a] Using the standard DSC equation $C_p = \langle \text{HF} \rangle / m \langle q \rangle$, where HF is the baseline and asymmetry corrected heat-flow rate, m the sample mass, and q the heating rate of the chosen segment of the complex sawtooth.

the measurements were not made consecutively. More detailed discussions of measurements with sapphire are found in [6].

Finally, the horizontals of the heat-flow rates for 0.6.785 mg of polystyrene as seen in Fig. 2 were also analyzed to yield heat capacities by standard DSC. The results are displayed in Table 4. The overall average value of the specific heat capacity is $1.356 \pm 3.6\%\,\text{J K}^{-1}\,\text{g}^{-1}$.

For an analysis of the instrument performance, Lissajous figures were recorded. Fig. 10 illustrates the Lissajous figure of the smoothed data for polystyrene shown in Figs. 2–5 (curve d). The not smoothed data are shown in Fig. 11 in an enlarged view. Both figures refer to modulation periods of 210 s. The different levels of the complex sawtooth correspond to the different rates of change of the sample temperatures (± 8, ± 4, ± 2 K min^{-1}). The coincidence of the five successive modulation cycles permits a discussion of the stationary states, and the spikes in Fig. 11 characterize the nonlinear responses. The consecutive numbers of the steps of the complex sawtooth modulation as given in Table 1 are marked in the figures. Note that each sub-cycle in the Lissajous

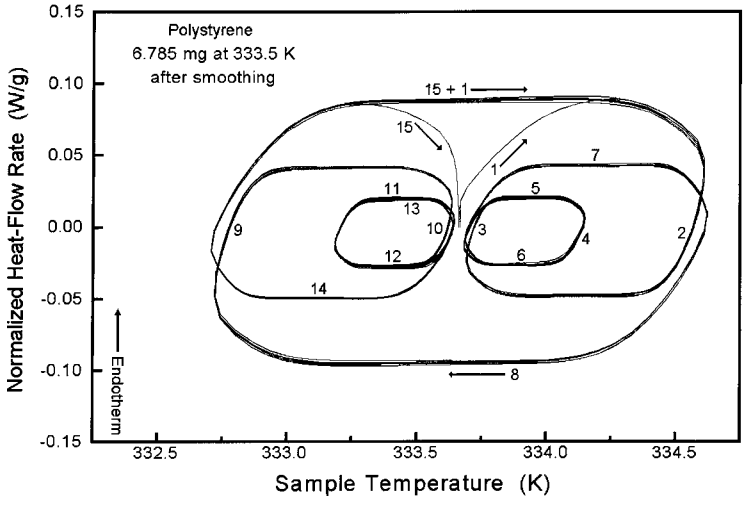

Fig. 10. Lissajous figure of the smoothed data of Fig. 2. The numerals indicate the segments listed in Table 1.

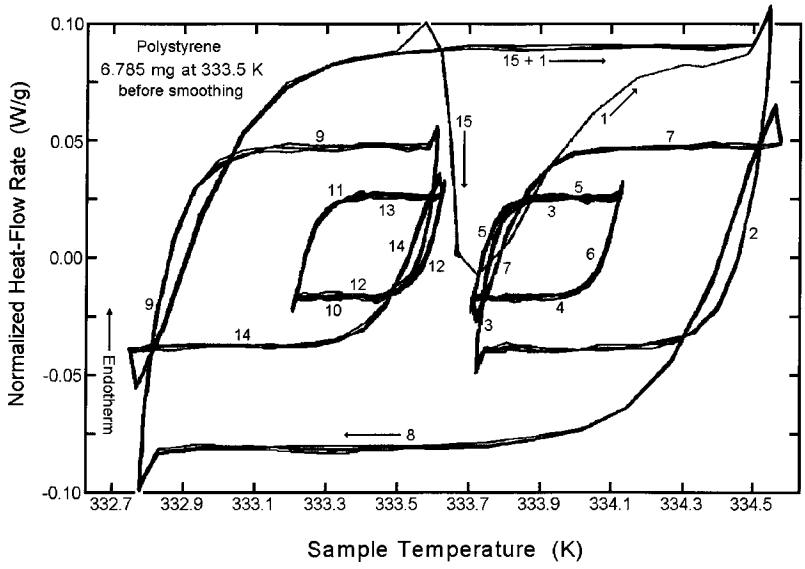

Fig. 11. Lissajous figure of the data as shown in Fig. 2 without smoothing. The numerals indicate the segments listed in Table 1. The presentation scale is double that of Fig. 10.

figure consists of two segments and takes 30 s, while one full cycle takes 210 s. Five full cycles are superimposed.

4. Discussion

The simple complex sawtooth of Table 1 and Fig. 1 can be generated with good repeatability, although rounded at the teeth, as is illustrated in Fig. 2b. A comparison of Eq. (2) and the amplitudes of Table 2 shows good agreement. In fact, by comparing different calorimeters, one can see that the closer the heater is to the temperature control, the closer one can match Fig. 1 and Eq. (2). The precise reproduction of the sawtooth, however, is not an important issue in multi-frequency modulation. The key issue is that the heat-flow response to the temperature changes can be described by a linear differential equation, such as the Fourier equation of thermal conductivity [10,11]. In this case the changes in the temperature profile lead to additive solutions of the overall differential equation, guaranteeing linearity between modulation of the T_S and the heat-flow response. It could be proven in [3] that for negligible temperature gradients within sample and reference pans and adherence to the Fourier equation, Eq. (1) describes the heat capacity, even if steady state is not reached. The value of τ is in this case C_r, the reference colorimeter heat capacity, divided by the Newton's-law constant K. The deviation from this limit must be due to temperature gradients within the calorimeters. This temperature gradient is naturally dependent on sample type, mass, and even on the positioning of the calorimeter pans, as was discussed in [4] and [6].

The spikes which are depicted in Fig. 2a whenever the heating rate changes, are detailed in the Lissajous representation in Fig. 11. They have no counterpart in the sawtooth of Fig. 2b, but occur over the time interval of rounding of the teeth, with the peaks near the maxima and minima of the temperature. A check of curve a in Fig. 3 which represents segments 5 and 6 of Table 1 shows that the sample temperature lags 3–4 s behind the program temperature.

Analyzing Fig. 11 in more detail and a comparison with curve a in Fig. 3 reveals that the maxima and minima of the sawtooth deviate from the set values of ± 1.0 and ± 0.5 K by -0.04 to -0.17 K. The overall Lissajous figure, however, is centrosymmetric, as can also be seen from the missing second harmonic of temperature and heat flow in Table 2. The sizes, types, and inabilities to reach the programmed extreme of the

sawtooth are strictly dependent on the heating rate, q and the anticipated change in the heating rate, Δq. The smaller the heating rate of the segment of the sawtooth, the smaller is the peak in the heat-flow rate. Peaks occurs at the ends of segments 1 and 9 where Δq is $1.5q$, sharp spikes at the ends of segments 5 and 11 where Δq is $2.0q$, and loops at the ends of segments 7 and 13 where Δq is $3.0q$. The changes at the ends of segments 1, 5, 7, 9, 11, and 13 and their centrosymmetric counterparts can be ordered in sequence of deviation from the programmed temperature by adding the sequence number in q (8, 4, 2 K min^{-1}) to half the sequence number in Δq (12, 6, 4 K min^{-1}). These regularities make it clear that the electronic circuitry does not image the changes in the temperature program, a property that makes the system nonlinear in the transition regions of the sawtooth.

The smoothing procedure shown in Fig. 3 eliminates the obvious spikes without significant influence on the total measured heat flow, as is also demonstrated in Fig. 10. In fact, it leads to a much closer match of the program timing (as marked in Fig. 3 for steps 5 and 6 in Table 1) than the data that are not smoothed. Figs. 4 and 5 reveal the sensitive nature of the change with smoothing of the correction factor τ. Close inspection of Fig. 5 indicates further that the smoothing affects the different segments of the complex sawtooth and introduces a small frequency dependence into τ. The effect seems, however, small since the extrapolation is rather short. Although smoothing is thus a reasonable procedure, it would increase precision to adjust the calorimeter to eliminate the peaks by improving the temperature control and short of this adjusting modulation amplitudes and frequencies.

The quality of the heat capacity data after correction for the different frequencies can be judged from Figs. 7 and 9. The standard deviations are between 0.5 and 0.7%. These values can be compared to the standard DSC values of Table 4 with a standard deviation of $\pm$3.6%. Considering that the measuring method has not been optimized as yet for sample mass and modulation amplitude, one can assume that measuring quasi-isothermally with the complex sawtooth may reach a precision of considerably better than 1%, sufficient to compensate for the higher effort needed to obtain the data. In particular, it can be seen from the analysis, that most of the computation steps can be included in the software for data analysis.

A final topic that will be investigated in the future is the question whether the analysis for τ can be extended to extract information on the frequency dependence of heat capacity as it is observed, e.g. in the glass transition region. For this purpose, the dependence of τ on temperature and frequency would have to be analyzed throughout the glass transition region to identify changes from the linear frequency dependence expected from the instrument effect. Measurements of this type would have the advantage of studying the identical material at different frequencies, which is not possible by separate, single sinusoidal experiments as were done earlier. In the latter case it is likely that different thermal histories are experienced in the separate runs.

5. Conclusions

It is shown that it is possible to measure heat capacity with simultaneously applied temperature modulations of different frequencies. The first results indicate that this method may increase the precision of measurement of heat capacity. Special problems with this method and their solution have been identified and indicate that the different type of DSCs need different analysis methods. It is hoped that this instrumentation will also be of help in the design of the next generation of temperature-modulated DSC.

Acknowledgements

This work was supported by the Division of Materials Research, National Science Foundation, Polymers Program, Grant No. DMR-9703692 and the Division of Materials Sciences, Office of Basic Energy Sciences, US Department of Energy at Oak Ridge National Laboratory, managed by Lockheed Martin Energy Research Corporation for the US Department of Energy, under contract number DE-AC05-96OR22464.

References

[1] P.S. Gill, S.R. Sauerbrunn, M. Reading, J. Therm. Anal. 40 (1993) 931.

[2] M. Reading, A. Luget, R. Wilson, Thermochim. Acta 138 (1994) 295.
[3] B. Wunderlich, A. Boller, I. Okazaki, K. Ishikiriyama, W. Chen, M. Pyda, J. Pak, I. Moon, R. Androsch, Thermochim. Acta 330 (1999) 21.
[4] R. Androsch, I. Moon, S. Kreitmeier, B. Wunderlich, Thermochim. Acta 357/358 (2000) 267.
[5] M. Reading, B.K. Hahn, B.S. Crowe, Method and Apparatus for Modulated Differential Analysis, US Patent 5 224 775, July 6, 1993.
[6] R. Androsch, B. Wunderlich, Thermochim. Acta 333 (1999) 27.
[7] B. Wunderlich, R. Androsch, M. Pyda, Y.K. Kwon, Thermochim. Acta 348 (2000) 181.
[8] D.G. Archer, J. Phys. Chem. Ref. Data 22 (1993) 1441.
[9] B. Wunderlich, Y. Jin, A. Boller, Thermochim. Acta 238 (1994) 277.
[10] A. Boller, Y. Jin, B. Wunderlich, J. Therm. Anal. 42 (1994) 307.
[11] W. Chen, M. Dadmun, G. Zhang, A. Boller, B. Wunderlich, Thermochim. Acta 324 (1998) 87.
[12] K. Ishikiriyama, B. Wunderlich, J. Therm. Anal. 50 (1997) 337.
[13] B. Wunderlich, Thermal Analysis, Academic Press, New York, 1990. For an update in form of the computer-course Thermal Analysis of Materials' 1999, see our web-site, found at the URL: http://web.utk.edu/~athas/courses/tham99.html
[14] U. Gaur, B. Wunderlich, Phys. Chem. Ref. Data 11 (1982) 313.